

In-flight diesel particulate matter removal using nonthermal plasma filtering

Haruhiko Yamasaki¹, Akihiro Shidara¹, Yuya Shimidzu¹, Tomoyuki Kuroki¹, Hak-Joon Kim², Masaaki Okubo^{1,*}

¹ Department of Mechanical Engineering, Osaka Prefecture University, Japan

² Department of Environmental Machinery, Korea Institute of Machinery and Materials, Republic of Korea

* Corresponding author: mokubo@me.osakafu-u.ac.jp (Masaaki Okubo)

Received: 26 October 2020

Revised: 19 December 2020

Accepted: 24 December 2020

Published online: 28 December 2020

Abstract

The concentration of particulate matter (PM), which is present in the atmosphere, is a major environmental problem in Korea and Japan. We propose a plasma filtering method for the removal of PM or nanoparticles in flight by direct plasma application to passing PM-containing gas. The method ensures that pressure-loss is low and does not require filter regeneration or cleaning. In this method, PM is removed by the chemical reactions and electrostatic precipitation effects associated with plasma by passing the PM-containing gas through a cylindrical plasma reactor containing surface discharge electrodes. The exhaust gas emitted from a diesel engine is diluted and introduced into the plasma reactor and the PM removal efficiency is investigated using a scanning mobility particle sizer (SMPS) apparatus. In order to examine the PM removal reactions in the reactor, the exhaust gaseous component concentrations of NO_x, NO, CO, and O₂ are measured. The results indicate that no PM is observed inside the reactor and an increase in CO is detected. The combustion removal of PM using the plasma is thus confirmed. A PM removal efficiency of more than 85% is achieved when 200–400 W of electrical input power is applied to the cylindrical plasma reactor and with an applied engine load of 0% and 25%. We demonstrated the possibility of the simultaneous reduction of PM and NO_x by adjusting the plasma processing conditions.

Keywords: Diesel particulate matter, nonthermal plasma, partial collection efficiency, NO_x.

1. Introduction

The concentration of particulate matter (PM), typified by PM_{2.5}, which is present in the atmosphere, is a major environmental problem in Korea and Japan. When it is inhaled through respiration, it is deposited in the lungs and adversely affects human health. Therefore, its reduction has gained international interest. Air cleaners that incorporate electrostatic precipitators and high-efficiency particulate air (HEPA) filters are effective for removing suspended PM in the atmosphere. PM can effectively be reduced by operating such air-cleaners indoors [1–3]. In other instances, for PM in the exhaust gas of diesel engines, a diesel particulate filter (DPF) is installed in the exhaust pipe as a measure to reduce PM generation at the source. Using a DPF, it is usually possible to collect particulates with a high efficiency of 95% or more. However, in removal methods that use ordinary filters, such as HEPA and DPF, the associated pressure loss is large. In addition, because blockages can occur during use, it is necessary to regularly clean, regenerate, and replace the filters used for PM removal [4–10].

In the present study, we propose a plasma filtering method that can remove PM in flight by applying plasma directly to passing PM-containing gas. In this method, PM is removed by the chemical reactions and dust collecting effects associated with plasma by passing PM-containing gas through a cylindrical plasma reactor containing surface discharge electrodes. Because the pressure loss and the performance deterioration during long-term operation are small, efficient, and continuous, PM removal can be performed without filter regeneration or cleaning. The reactor also has the effect of removing nitrogen oxides (NO_x = NO + NO₂), odors, and volatile organic compounds (VOCs)-containing gases. The objective of the present study is to conduct

international collaborative research on a plasma system that can provide a large filtering volume, improve the residence time characteristics of radicals, and increase the decomposition performance of the system.

Collaborative groups have been conducting joint research to investigate the basic PM removal characteristics of plasma filters through international exchange based on the 2014 academic exchange agreement between Osaka Prefecture University (OPU) and the Korea Institute of Machinery and Materials (KIMM). Suspended PM in the atmosphere is generated from artificial sources, such as combustion boilers in thermal power plants, automobile and ship engines, and combustion equipment in factories. Complete removal by plasma has been confirmed in previous studies for combustible PM components, such as dry soot, for the soluble organic fraction, and for hydrocarbon compounds [11–20]. Furthermore, noncombustible components of PM are collected inside the device by virtue of the electrostatic precipitation effect. Although it is necessary to clean the inside of the reactor regularly, most of the PM is burned and removed. As a result, cleaning is required less frequently than for filters.

We install a plasma reactor energized by a high-voltage high-frequency power supply and attempt a new test. The aim of the study is to develop a plasma aftertreatment system for practical use as a PM aftertreatment technology that complies with future exhaust gas regulations. In this experiment, the PM removal performance is investigated by performing an efficient surface discharge for radical species generation. In addition, to examine the PM removal reactions in the reactor, the exhaust gas component concentrations of NO_x , NO, CO, and O_2 are measured simultaneously. As a result, an increase in CO_x (i.e., $\text{CO} + \text{CO}_2$) is detected, and PM combustion removal by plasma [21, 22] is confirmed. We also show the possibility of the simultaneous removal of PM and NO_x [23, 24] using PM as a reducing agent for NO_x .

2. Experimental

2.1 Surface-discharge-type plasma reactor

Fig. 1 shows schematics and a photograph of the nonthermal plasma (NTP) reactor and power source for in-flight diesel particulate matter removal. Fig. 1 (a) shows a side view schematic of the NTP reactor and a cross-section with the discharge electrodes. The NTP reactor used in this experiment (Surface-discharge-induced Plasma Chemical Process (SPCP) discharge tube: OC70/AC, Masuda Research Inc.) is a cylindrical surface discharge type with an outer diameter of 80 mm, an inner diameter of 68 mm, an outer length of 300 mm, and an inner length of 280 mm. It is manufactured using a high-purity alumina ceramic tube. The residence time in the plasma reactor is 12.2 s when the flow rate of the exhaust gas is 5 L min^{-1} . A discharge electrode is provided on the inner surface of the ceramic inside the tube, and an induction electrode is provided inside the ceramic, as shown in the cross-section in Fig. 1 (a). When an AC-pulsed high voltage is applied between the two electrodes, a surface discharge extends from the discharge electrode along the ceramic wall. As a result, NTP is generated on the surface of the discharge electrode and some radical species and electrons are induced. PM in the exhaust gas flow that comes into contact with this is oxidized to CO_x . In addition, air-cooling fins are installed on the outside of the ceramic tube to prevent overheating of the reactor by dissipating heat. Fig. 1 (b) shows the plasma reactor and power supply installation. The apparatus consists of an AC pulsed high-voltage power supply (HCII-70/2, input: voltage = three-phases 200 Vac, power = 1.5 kVA (50/60 Hz), output: peak-to-peak voltage = 14 kV (no electrical load), input power = 70–860 W, frequency = 9.9 kHz, Masuda Research Inc.) that matches the surface discharge tube. In this type of surface discharge reactor, the space filled with plasma-induced radical species is larger than that in dielectric barrier discharge reactor. Therefore, higher efficiency in-flight PM removal could be possible with the species. When the present technology is applied to actual automobile, similar-type AC pulse high voltage power supply energized by an automobile battery can be used. The present plasma reactor is made of alumina ceramics, plastics, and steel. The reactor is robust because in automobile such ceramics is usually used for catalysts.

2.2 Reactions of Particulate Matter and NO_x

Diesel emission PM mostly consists of dry soot (carbon, C), a soluble organic fraction (SOF), hydrocarbon compounds (HCs), nitrates, and sulfates [1]. In the proposed method, these PMs first pass through the plasma reactor and stay inside during residence time. Next, NTP-induced radicals and active species, such as the

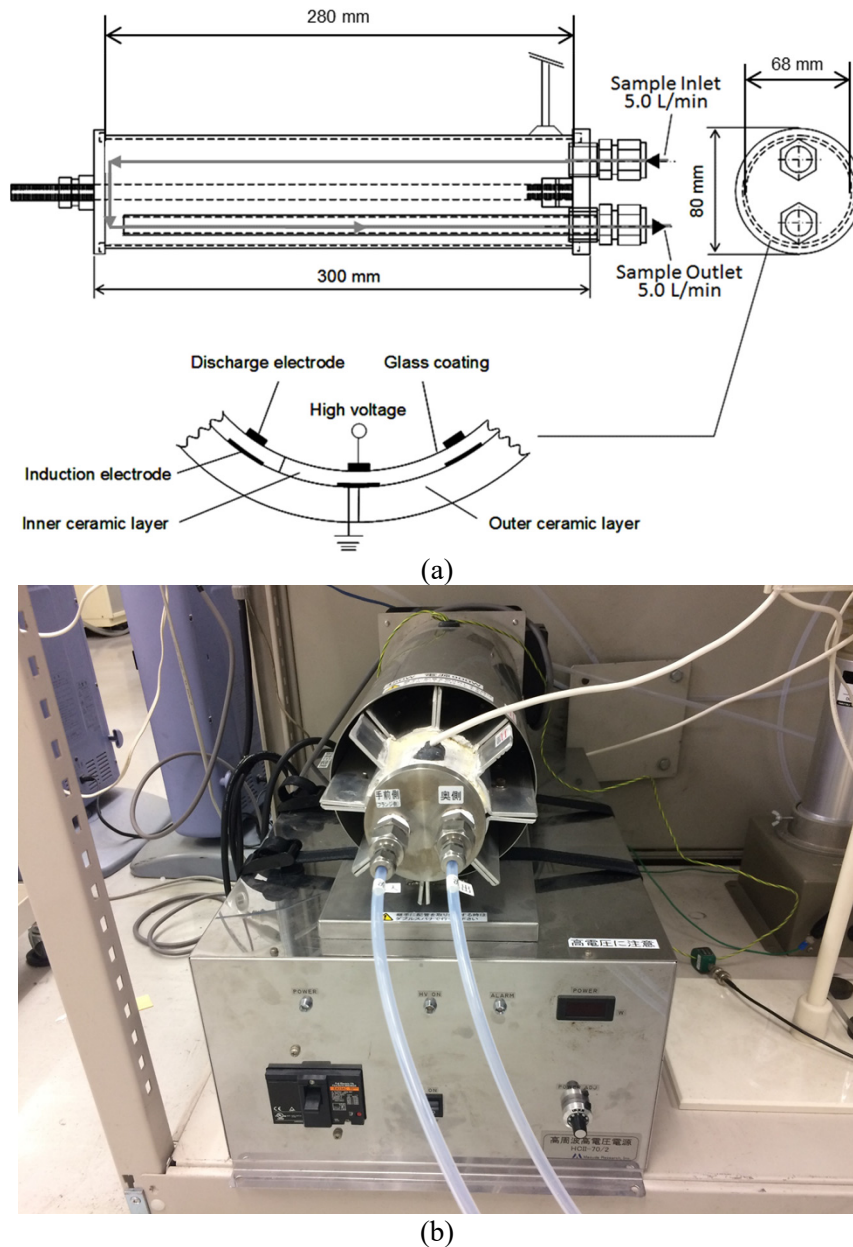


Fig. 1. Schematics and photograph of the nonthermal plasma reactor (NTP) and the power source for in-flight diesel particulate matter removal. (a) Schematics of the side view of the NTP reactor and a cross section showing the discharge electrodes. (b) Installation showing the plasma reactor and power supply.

oxygen radicals O, NO₂, and O₃, react with the combustible PMs (C, SOF, and HCs) to be oxidized and to induce gaseous CO_x. As a result, in-flight PM treatment can be performed. The main chemical reactions involved in PM combustion removal are shown in (1) – (9).





where m and n are integers. It is noted that oxygen radical O is induced mainly by the thermal decomposition of O_3 and NO_2 . The typical reaction temperature is 200–300 °C. As shown in reactions (1)–(9), NO_2 and O_3 originally contribute to the oxidation of PM. PM is collected inside the plasma system by virtue of electrostatic precipitation effects and is removed in-flight by combustion as described in (1)–(9).

2.3 Experimental setup and method

Fig. 2 shows the experimental setup used for testing the PM treatment system incorporating surface discharge. Fig. 2(a) shows a schematic diagram of the experimental setup for the PM treatment system. Fig. 2(b) shows an overview of the diesel engine generator, exhaust piping, and sampling port. In Fig. 2(a), the exhaust gas emitted from a diesel engine generator (KDE2.0E, light oil fuel, single-cylinder, direct injection, rotational speed = 3600 rpm, displacement volume = 211 mL, output = 2 kW, exhaust flow rate = 380 NL min⁻¹, Wuxi KIPOR Power Co. Ltd., China), which is provided with an electrical heating load, is divided at the sampling port to provide a flow rate of 2.5 L min⁻¹, which in turn is diluted with $\text{N}_2 + \text{O}_2$ cylinder gas ($\text{N}_2 = 90\%$ and $\text{O}_2 = 10\%$) at a flow rate of 2.5 L min⁻¹, as measured using flow meter A (RK1710 Series KOFLOC Corp.). The oxygen concentration of the diluted gas is set to a value similar to the oxygen concentration of the engine exhaust gas, which is approximately 10%. The diluted gas is flowed using a pump (APN-S085LVX1-1, IWAKI Co., Ltd.) and the flow rate is adjusted to 5.0 L min⁻¹ by using flow meter B. PM treatment is performed by passing the gas through the plasma reactor. Because the NTP-treated exhaust gas contains ozone generated in the reactor, which may corrode the measuring instruments, it is first passed through a tubular furnace (KPO-14 K, Isuzu Seisakusho Co., Ltd.) installed immediately after the reactor. The decomposition of ozone is performed at a set temperature of 300 °C. Next, flow meter C is used to adjust the sample to a flow rate of 0.5 L min⁻¹. The sampled gas is diluted 10-fold with N_2 cylinder gas at a flow rate of 4.5 L min⁻¹, which is adjusted using flow meter D. Using a scanning mobility particle sizer (SMPS), which is a combination of a differential mobility analyzer (DMA, Model 3080, TSI Inc.) and a condensation particle counter (CPC, Model 3787, TSI Inc.), the partial removal efficiency is measured for a particle size range of 30–500 nm, and the performance of the treatment system is evaluated. Dilution is performed with N_2 gas so as not to exceed the SMPS-measurable particle concentration. The concentrations of the gaseous components of NO, NO_x , CO, CO_2 , and O_2 in the 4.5 L min⁻¹ exhaust gas, which is adjusted using flow meter E, are measured using a gaseous concentration meter (PG-240, Horiba Ltd.). Furthermore, waveforms of current, voltage, and instantaneous power in the reactor are measured using a digital oscilloscope (DLM3054, Yokogawa Electric Corporation) fitted with a voltage divider (HV-P60, sensitivity = 1 V/2 kV, Iwatsu Electric Co., Ltd.) and a current probe (Model 2878, sensitivity = 0.1 V/1 A, Pearson Electronics, Inc.). The exhaust gas temperature and the reactor surface temperature are measured using thermometers A and B, respectively, which are fitted with thermocouples. Thermometer A indicates that the average exhaust gas temperature is 143 °C when an engine load is not added, and 172 °C when an engine load of 25% is added. Thermometer B indicates that the temperature at the NTP reactor outer wall is 24 °C for an input power of 100 W, 24 °C for an input power of 200 W, 30 °C for an input power of 300 W, and 39 °C for an input power of 400 W. For each power value from 100–400 W, the power is turned on for 5 min and off for 5 min, and then three PM removal efficiency data are obtained during a 30 min period. Because the sampling gas flow rate tends to decrease with the passage of time, the flow meter is adjusted to reach the set flow rate. The SMPS measurement time takes 2 min within a 5 min period. We also compare the reactor removal performance without an added diesel engine generator load (load = 0% or 0 W) and with an added 25% diesel engine generator load (load = 25% or generator power = 500 W).

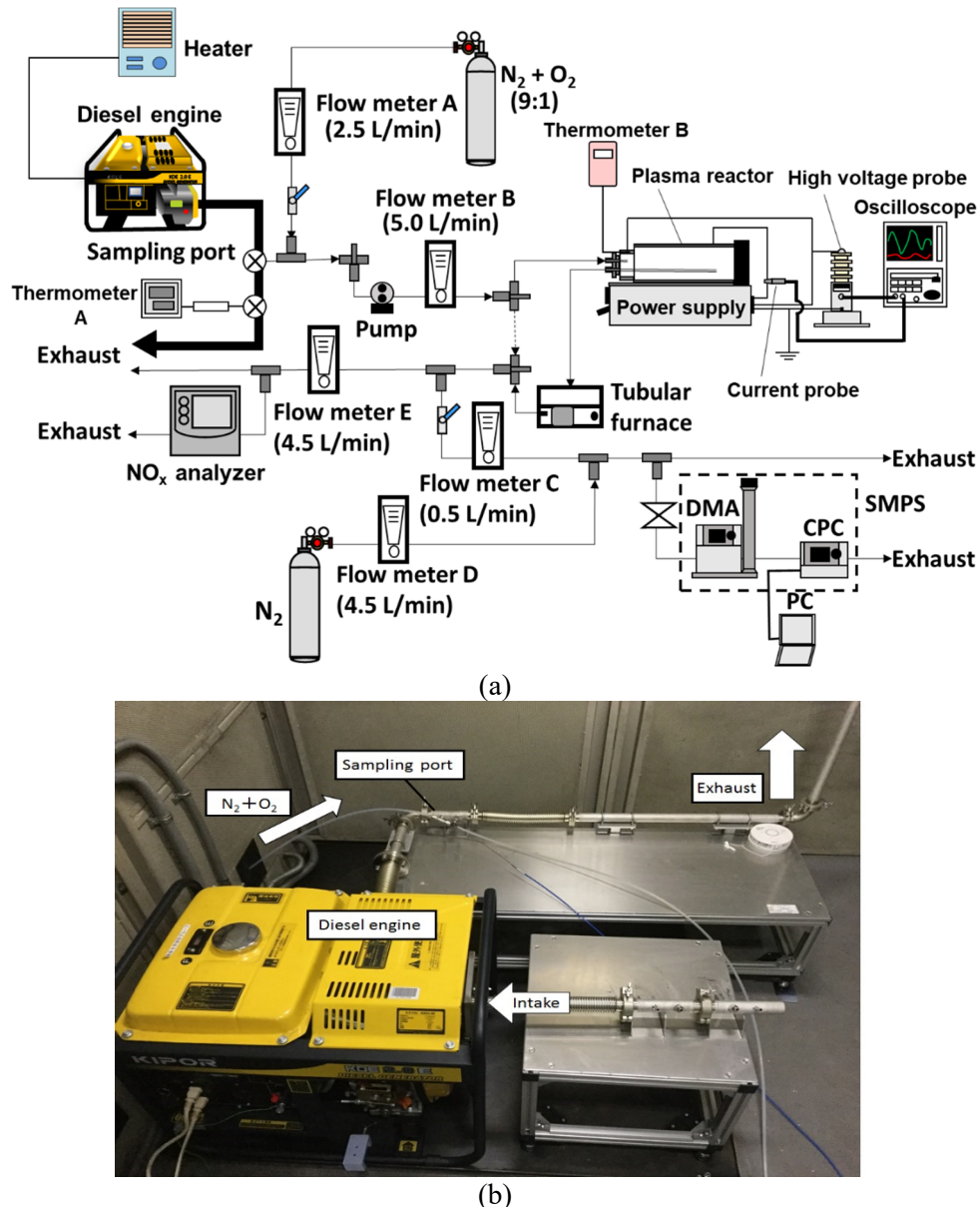


Fig. 2. Experimental setup used for testing the PM treatment system. (a) Schematic diagram of the experimental setup for the PM treatment system. (b) Overview of the diesel engine generator, exhaust piping, and sampling port.

3. Results and discussion

3.1 PM removal characteristics

Figs. 3 and 4 show typical waveforms obtained from the plasma reactor by electrical measurement using a digital oscilloscope for 0% engine generator load (load = 0%) and 25% engine generator load (load = 25%), respectively. In the figures, the horizontal axis represents time and the vertical axis is V , I , and $V \times I$, where V represents voltage, I represents current, $V \times I$ represents instantaneous power, and the plasma reactor input power is varied from 100 to 400 W. It can be seen from both figures that the kind of pulsed current and power waveforms that characterize dielectric barrier discharges or surface discharges are clearly observed when the input power is greater than 200 W. In addition, the peak current and power values for the load of 25% are greater than those for the load of 0%. The current becomes larger because the amount of moisture in the exhaust gas component is larger when the load is added, and both surface and volume resistivities of the alumina dielectric decrease under high humidity conditions.

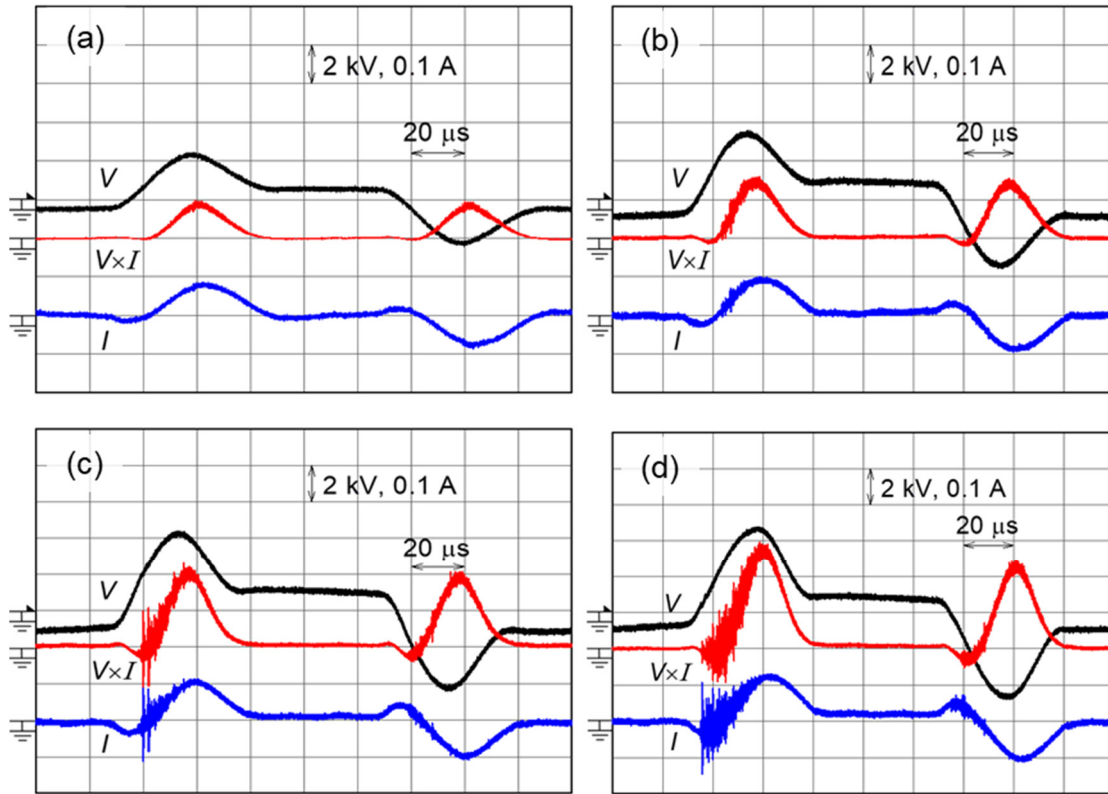


Fig.3. Typical waveforms obtained by electrical measurement performed on the plasma reactor using a digital oscilloscope with 0% engine generator load (load = 0%). (a) Input power = 100 W, (b) 200 W, (c) 300 W, and (d) 400 W.

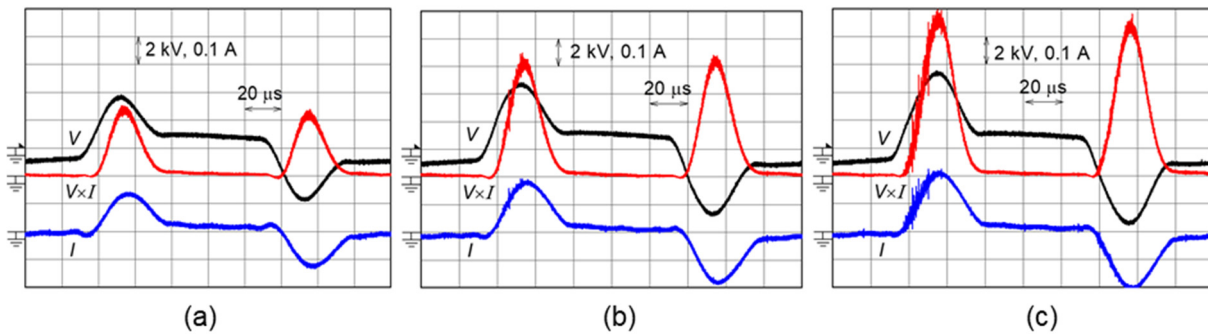


Fig.4. Typical waveforms obtained by electrical measurement performed on the plasma reactor using a digital oscilloscope with 25% engine generator load (load = 25%). (a) Input power = 200 W, (b) 300 W, and (c) 400 W.

3.2 PM removal characteristics

3.2.1 Cases with 0% engine load

Fig. 5 shows the distribution of averaged particle diameter-dependent number concentrations before and after the plasma treatment for reactor input power values of 100–400 W without an added engine load (load = 0%). The SMPS measurement result is shown in the figure. The horizontal axis represents the particle diameter, which is defined as the electrostatic mobility diameter or Stokes diameter (nm). The vertical axis represents the number concentration $dN/d\log D_p$ (cm^{-3}). The plot marked by white circles and noted as untreated, shows the result before plasma treatment, whereas the plots marked by solid symbols show the result for each power

value after plasma treatment. Furthermore, for each data point, the symbol represents the average value of three measured values. The sampling flow rate is $Q = 5 \text{ L min}^{-1}$. In the figure, the peak of the number concentration distribution before the treatment is associated with a particle size range of 60 to 70 nm. In addition, although it can be seen that the removal performance is superior when the input power is 200 to 400 W, the removal performance is inferior when the input power is 100 W. Because sufficient discharges do not occur at 100 W, the particle collection effect does not work effectively.

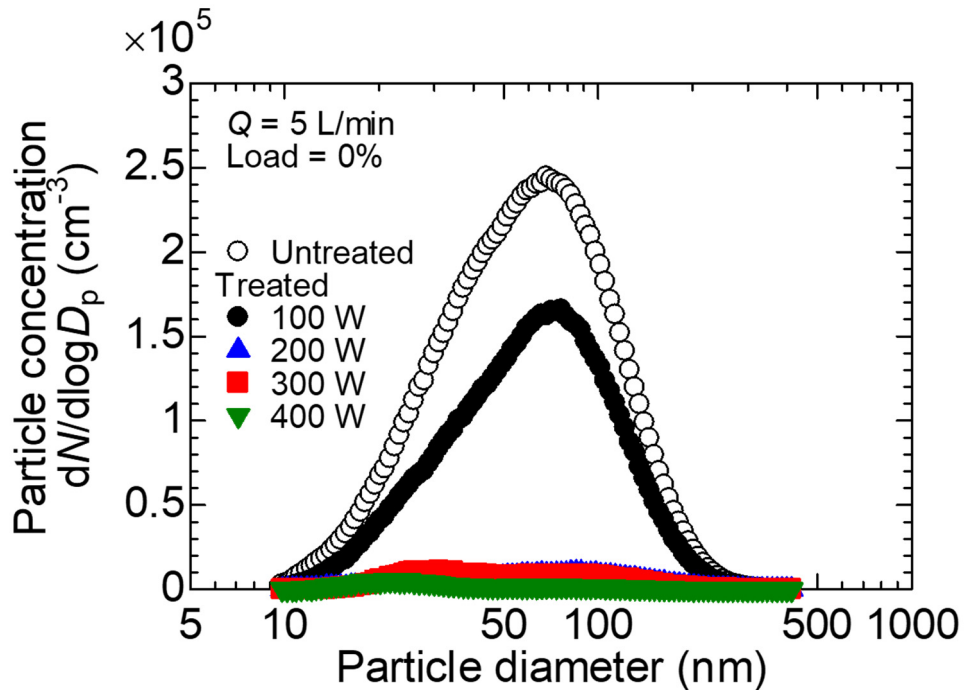


Fig.5. Distribution of averaged particle diameter-dependent number concentrations before and after the plasma treatment for a reactor input power of 100–400 W without an added engine load (load = 0%).

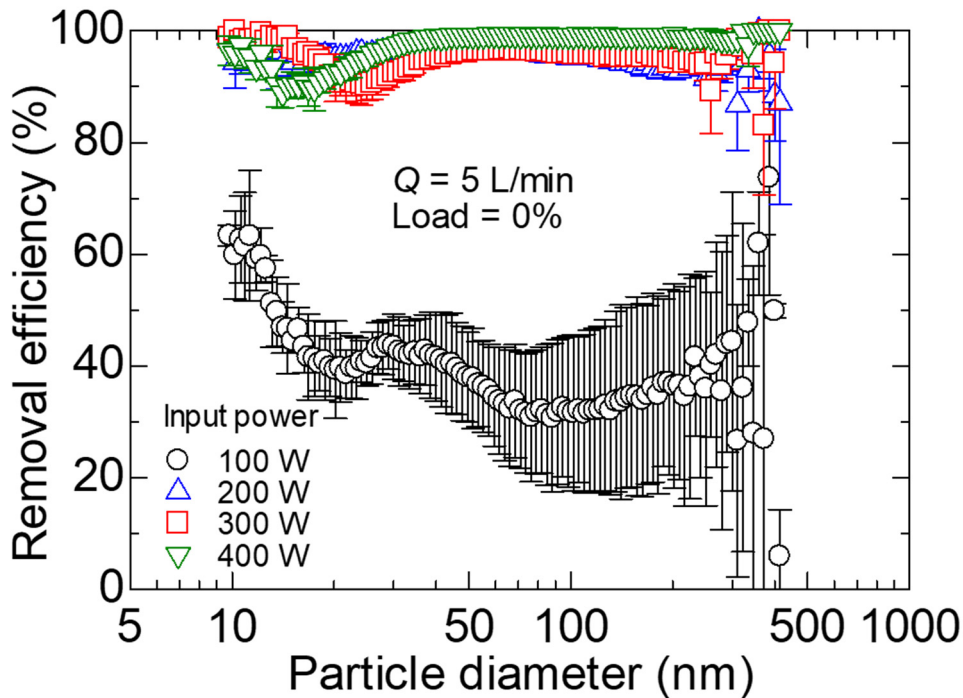


Fig.6. Particle-diameter dependent removal efficiency after the plasma treatment for a reactor input power of 100–400 W without an added engine load (load = 0%). The measurement error bars represent $\pm \sigma$.

Fig. 6 shows the particle diameter-dependent removal efficiency after the plasma treatment for reactor input power values of 100–400 W without an added engine load (load = 0%). The horizontal axis represents the particle diameter (nm) and the vertical axis represents the partial removal efficiency (%) of the number of particles. The specific input energy or energy density values are 333–1330 Wh m⁻³ (1.2–4.8 kJ L⁻¹). Furthermore, for each data point, the symbol represents the average value of three measured values, and the error bar represents $\pm \sigma$ (σ standard deviation). When the input power of the plasma reactor is 200 W or higher, the PM removal efficiency increases by more than 85%. Particles with a particle diameter in the range of 5 to 50 nm are called nucleation-mode particles, whereas particles with particle sizes in the range of 50 to 1000 nm are called accumulation mode particles. As shown in the figure, the nucleation-mode particle removal efficiency tends to decrease when the input power is 300 and 400 W. Although this phenomenon has not been elucidated, the possible reason is shown here. The plasma decomposes carbon particles with larger particle size into nucleation-mode particles with smaller particle size. The decomposition becomes more significant as the input power increases. Because the nucleation-mode particles are generated in the reactor, the removal efficiency decreases for higher input power. For accumulation mode particles, the removal efficiency tends to decrease for larger particles with decreasing input power. However, when the input power is 400 W, the removal efficiency is almost 100% for the accumulation mode particles, and a good removal performance of 90% or more is exhibited over the entire particle diameter range.

3.2.2 Cases with 25% engine load

Fig. 7 shows the distribution of averaged particle diameter-dependent number concentrations before and after the plasma treatment for reactor input power values of 200–400 W with an added engine load of 25% (load = 25% or generator power = 500 W). The horizontal axis, vertical axis, number of measurements, and sampling flow rate are all identical to those used in Fig. 5. Additionally, in the result obtained for 100 W, the number increases after the treatment. Therefore, it is considered that removal is not successful in this instance. This result is excluded from the figure and the following consideration. It can be seen from the figure that the peak in the number concentration distribution of particles before the treatment is associated with a particle size range of 40 to 50 nm. Compared to Fig. 5, the particle size range associated with the peak value decreases. This is caused by a rise in the combustion temperature due to the load on the engine, which causes the number of volatile particles covering the surface of the particles in the exhaust gas to decrease and the ratio of nucleation-mode particles to increase.

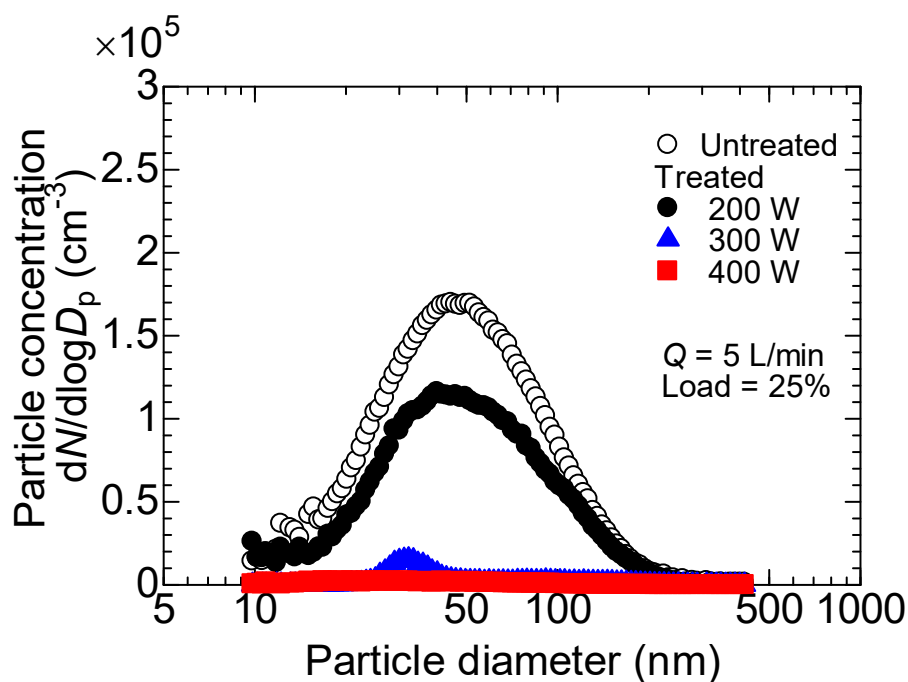


Fig.7. Distribution of averaged particle diameter-dependent number concentrations before and after the plasma treatment for a reactor input power of 200–400 W with an added engine load of 25% (load = 25% or generator power = 500 W).

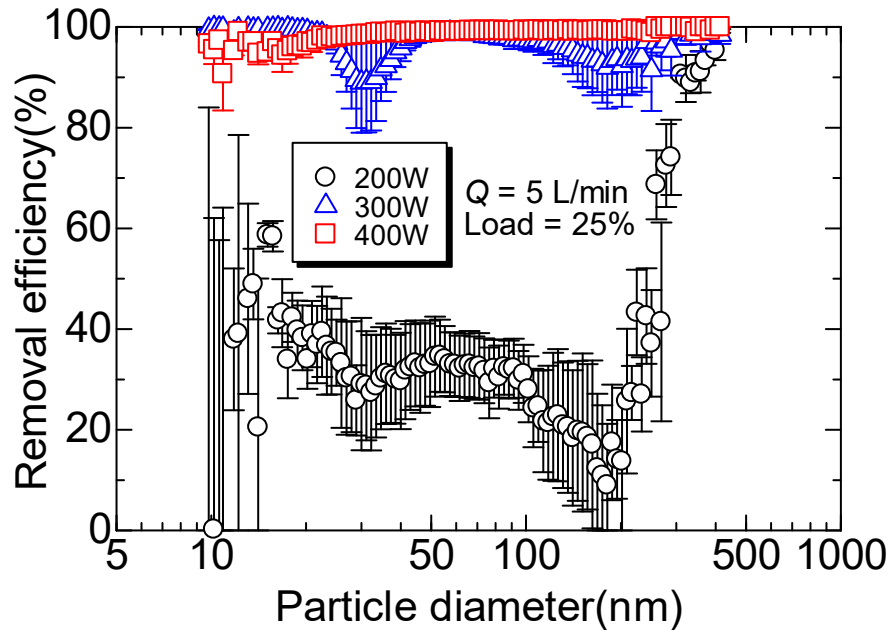


Fig.8. Particle diameter-dependent removal efficiency after the plasma treatment for a reactor input power of 200–400 W with an added engine load of 25% (load = 25% or generator power = 500 W). The measurement error bars represent $\pm \sigma$.

Fig. 8 shows the particle diameter-dependent removal efficiency after the plasma treatment for reactor input power values of 200–400 W with an added engine load of 25% (load = 25% or generator power = 500 W). The horizontal axis, vertical axis, number of measurements, data error bars, and sampling flow rate are similar to those present in Fig. 6. It can be confirmed from the figure that the removal efficiency becomes higher than 85% at 300 W and 400 W. However, it is found that for the particle size range of 10–40 nm, the nucleation-mode particle removal efficiency is lower. At 200 W, the removal efficiency drops to 50% or less, except for some particle size ranges. The removal efficiency is 85% or more at 300 W and 90% or more at 400 W, demonstrating good removal performance.

Fig. 9 shows a photograph of the vicinity of the electrodes taken inside the reactor after the completion of the experiment using an endoscope (digital industrial endoscope, DYKEISS Co.). The black lines correspond to the discharge electrodes. It is observed that the part near each electrode looks white as a result of PM removal, whereas the center part between the electrodes is slightly black. Because no particles are noted as remaining in the reactor, it confirms that the main particles are burned off.



Fig.9. Endoscope photograph of the area near the electrodes taken inside the reactor after completion of the experiment.

3.3 Gaseous component characteristics

Fig. 10 (a) and (b) show the measurement results for the exhaust gas component concentrations associated with a reactor input power of 100–400 W (a) when the engine load is absent (load = 0%) and (b) when an engine load of 25% is added (load = 25%). The horizontal axis represents the input power (W); the left vertical axis represents the gaseous concentrations of NO_x, NO, and CO; and the right vertical axis represents the gaseous concentrations of O₂ and CO₂. For each data point, the symbol represents the average value of the three measured values, and the error bars represent $\pm 0.5 \sigma$. Averaged initial concentrations at a reactor input power of 0 W are NO = 108 ppm, NO_x = 116 ppm, CO = 444 ppm, CO₂ = 1.50%, and O₂ = 14.54% for the load of 0%, and NO = 166 ppm, NO_x = 176 ppm, CO = 417 ppm, CO₂ = 2.17%, and O₂ = 14.24% for the load of 25%. It can be seen from the two graphs that no significant change is observed in any gas component at 100 W for the load of 0% as shown in Fig. 10 (a), and at 200 W or less for the load of 25% as shown in Fig. 10 (b).

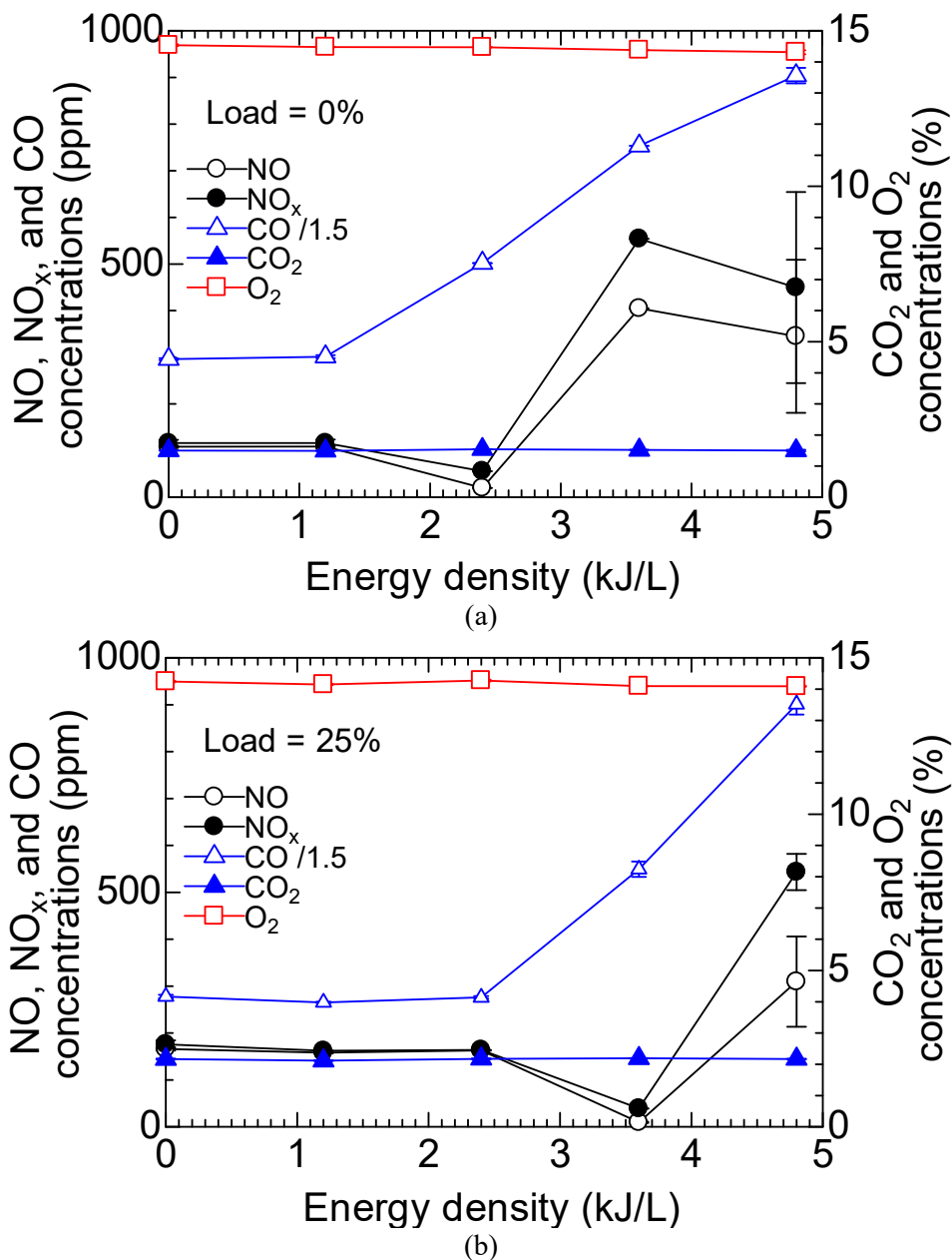


Fig.10. Exhaust gas component concentration measurement results for a reactor input power of 100–400 W or energy density of 1.2–4.8 kJ/L (a) without an added engine load (load = 0%) and (b) with an added engine load of 25% (load = 25% or generator power = 500 W). The measurement error bars represent $\pm 0.5 \sigma$.

This is consistent with the results for the removal efficiency as shown in Fig. 6 and Fig. 8, which are reduced under the specified power values. Therefore, in each case, it is considered that the plasma has little effect on plasma reactions. The CO concentration increases at 200 W or higher, whereas NO_x and NO concentrations vanish at 200 W for the load of 0% and at 300 W for the load of 25%. This is due to the active oxygen, ozone, and nitrogen dioxide that are generated in the reactor being used to react with C in the PM components, based on reactions (1)–(5), (8), and (9). CO increases, in other words, PM is oxidized and combusted at a low temperature of less than 50 °C. Although the rise in CO₂ is small to detect with the gaseous analyzer because the background concentration of CO₂ is higher (~2%) than CO, averaged CO₂ increase is approximately 0.03% = 300 ppm at 200 W or higher for the load of 0% and 0.01% = 100 ppm at 300 W or higher for the load of 25%. In addition, it is considered that the NO_x component in the exhaust gas is removed by the reaction with PM under the conditions of 200 and 300 W, as shown in Fig. 10 (a) and Fig. 10 (b), respectively. In reactions (9) and (10), C in PM acts as a reducing agent to remove NO_x. These processes contribute to the result that is obtained, as shown in the figure. The energy efficiencies (namely, ratio of the removed mass to the NTP energy) for the NO_x reduction are estimated as 0.20 g(NO₂) kWh⁻¹ at 200 W for the load of 0%, and 0.31 g(NO₂) kWh⁻¹ at 300 W for the load of 25% with the present system. It is noted that the unit of g(NO₂) is an equivalent mass of NO_x based on the molecular weight of NO₂. These values are still lower compared to our previous data (4.3 g(NO₂) kWh⁻¹) with the single-stage reduction system [23]. On the other hand, 60% of the engine total power is required for 85% PM removal for the load of 25%. This power is much higher compared to our previous data (5% of the engine total power) with the DPF regeneration system [1]. The performances should be improved further in a future work. With higher input power, NO_x is increased by the application of plasma and with the increase in input power. This may be caused by OH radicals generated by reactions associated with the moisture in the reactor [25]. When OH reacts with nitrogen, NO_x is induced at room temperature, in a similar manner to that described by the extended Zeldovich mechanism.

It can be seen from these results that when PM is removed from the exhaust gas, the removal efficiency generally increases with an increase in the input power. However, NO_x in the exhaust gas also tends to increase alongside this. Therefore, it is clarified that the input power needs to be adjusted appropriately so that NO_x emission can be suppressed. NO_x increases should be suppressed, and simultaneous NO_x and PM should be realized at the cost of lower PM collection efficiency. CO_x increase is unavoidable as a result of PM combustion. Swirl or azimuthal flow inside the reactor could increase the residence time and collection efficiency of the reactor at the lower power. The ultimate goal would be to realize a total exhaust gas purification system for diesel engines used in the automobile and ship industries that combines plasma filter technology and exhaust gas component recirculation technology [1]. To perform high-efficiency PM processing in engines installed in transportation equipment such as ships and automobiles, the power of the plasma reactor should be appropriately controlled according to the engine load. Even at higher engine load, PM concentration in the exhaust gas is almost in the same order. Therefore, it is considered that the result at higher engine load will be similar to the present ones. However, in future research the result should be confirmed experimentally. The present paper reports a basic study, and first confirms that NTP in-flight DPM removal is possible. In future research the effect of flow rate on PM removal should be examined in detail. Especially, experiments with higher flow rate of the gas are needed on to obtain the solution for scalability of the treatment system.

4. Conclusion

PM removal efficiency is evaluated by passing exhaust gas through a plasma reactor driven by surface discharge. In addition, the reactions in the reactor are investigated by measuring the exhaust gas components before and after plasma treatment. In the future, we will continue our research by conducting further experiments under various conditions with the goal of building a system for diesel engines that can simultaneously and more efficiently remove PM and NO_x. The main results obtained in this study are summarized as follows:

(1) When the load to the diesel engine is 0% and the input power of the plasma reactor is 200 W or higher, the PM removal efficiency increases to more than 85%. When the input power is 400 W, the removal efficiency rises to almost 100% for the accumulation mode particles, and a good removal performance of 90% or more is exhibited over the entire range of diameters. From the exhaust gas concentration analysis results, the NO_x

and NO concentrations can be reduced at 200 W, but the NO_x and NO concentrations increase at 300 W and higher. Because of PM combustion, the CO_x concentration increases at 200 W or higher.

(2) When the load to the diesel engine is 25% and the input power is set to 300 W or higher, the PM removal efficiency increases to more than 85%. The removal efficiency is 90% or more at 400 W, demonstrating good removal performance. From the exhaust gas concentration analysis results, it is found that the NO_x and NO concentrations can be reduced at 300 W. However, the NO_x and NO concentrations increase at 400 W and higher. Because of PM combustion, the CO_x concentration increases at 300 W or higher.

(3) The experimental results indicate that when removing PM from the exhaust gas of a diesel engine, the removal effect increases with increasing input power. However, pollutants such as NO_x and NO in the exhaust gas will also increase. NO_x reduction is confirmed for an input power and engine load of 200 W and 0%, respectively, and 300 W and 25%, respectively. Therefore, it is necessary to adjust the reactor input power to the point at which NO_x and NO emissions are suppressed. To install this system into an engine used in a transportation system such as a ship or automobile, it will be necessary to adjust the electrical reactor power accordingly, based on the engine load.

Acknowledgment

We would like to thank Souta Hirano (graduate student at OPU) for his cooperation in the experiment. This research was supported by the Heiwa Nakajima Foundation, 2019 International Academic Research Grant. This international joint research involving KIMM and OPU is truly meaningful in terms of revitalizing our laboratories through personnel exchange. We appreciate the program and will continue to encourage international interaction between young researchers and graduate students.

References

- [1] Okubo M. and Kuwahara, T., *New Technologies for Emission Control in Marine Diesel Engines*: Butterworth-Heinemann, imprint of Elsevier, 2019.
- [2] Kim H.J., Kim M., Han B., Woo C.G., Zouaghi A., Zouzou N., and Kim Y.J., Fine particle removal by a two-stage electrostatic precipitator with multiple ion-injection-type prechargers, *J. Aerosol Sci.*, Vol. 130, pp. 61–75, 2019.
- [3] Kim M., Lim G.T., Kim Y.J., Han B., Woo C.G., and Kim H.J., A novel electrostatic precipitator-type small air purifier with a carbon fiber ionizer and an activated carbon fiber filter, *J. Aerosol Sci.*, Vol.117, pp. 63–73, 2018.
- [4] Okubo M., Arita N., Kuroki T., Yoshida K., and Yamamoto T., Total diesel emission control technology using ozone injection and plasma desorption, *Plasma Chem. Plasma Process.*, Vol. 28 (2), pp. 173–187, 2008.
- [5] Yao S., Kodama S., Yamamoto S., and Fushimi C., *Asia-Pacific J. Chem. Eng.*, Vol. 5 (5), pp. 701–707, 2009.
- [6] Babaie M., Davari P., Talebizadeh P., Zare F., Rahimzadeh H., and Ristovski Z., *Chem. Eng. J.*, Vol. 276 (2), pp. 240–248, 2015.
- [7] Pu X., Cai Y., Shi Y., Wang J., Gu L., Tian J., and Fan R., Carbon deposit incineration during engine flameout using non-thermal plasma injection, *Int. J. Automotive Technol.*, Vol. 19, pp. 421–432, 2018.
- [8] Ranji-Burachaloo H., Masoomi-Godarzi S., Khodadadi A. A., and Mortazavi Y., Synergetic effects of plasma and metal oxide catalysts on diesel soot oxidation., *Appl. Catal. B: Environmental*, Vol. 182, pp. 74–84, 2016.
- [9] Ji L., Cai Y., Shi Y., Fan R., Wang W., and Chen Y., Effects of nonthermal plasma on microstructure and oxidation characteristics of particulate matter, *Env. Sci. & Tech.*, Vol. 54 (4), pp. 2510–2519, 2020.
- [10] Kuwahara T., Nakaguchi H., Kuroki T., and Okubo M., Continuous reduction of cyclic adsorbed and desorbed NO_x in diesel emission using non-thermal plasma, *J. Hazardous Mater.*, Vol. 308, pp. 216–224, 2016.
- [11] Kuwahara T., Nishii S., Kuroki T., and Okubo M., Complete regeneration characteristics of diesel particulate filter using ozone injection, *Appl. Energy*, Vol. 111, pp. 652–656, 2013.
- [12] Lin H., Huang Z., Shangguan W., and Peng X., Temperature-programmed oxidation of diesel particulate matter in a hybrid catalysis-plasma reactor, *Proc. Combust. Inst.*, Vol. 31 (2), pp. 3335–3342, 2007.
- [13] Babaie M., Davari P., Zare F., Rahman M., Rahimzadeh H., Ristovski Z., and Brown R., Effect of pulsed power on particle matter in diesel engine exhaust using a DBD plasma reactor, *IEEE Trans. Plasma Sci.*, Vol.

- 41 (8), pp. 2349–2358, 2013.
- [14] Babaie M., Kishi T., Arai M., Zama Y., Furuhashi T., Ristovski Z., Rahimzadeh H., and Brown R., Influence of non-thermal plasma after-treatment technology on diesel engine particulate matter composition and NO_x concentration, *Int. J. Env. Sci. Tech.*, Vol. 13, pp. 221–230, 2016.
- [15] Shi Y., Cai Y., Fan R., Cui Y., Chen Y., and Ji L., Characterization of soot inside a diesel particulate filter during a nonthermal plasma promoted regeneration step, *Appl. Therm. Eng.*, Vol. 150, pp. 612–619, 2019.
- [16] Wang P., Gu W., Lei L., Cai Y., and Li Z., Micro-structural and components evolution mechanism of particulate matter from diesel engines with non-thermal plasma technology, *Appl. Therm. Eng.*, Vol. 91, pp. 1–10, 2015.
- [17] Fan R., Cai Y., Shi Y., and Cui Y., Effect of the reaction temperature on the removal of diesel particulate matter by ozone injection, *Plasma Chem. Plasma Process.*, Vol. 39 (8), pp. 143–163, 2019.
- [18] Gu L., Cai Y., Shi Y., Wang J., Pu X., Tian J., and Fan R., Effect of indirect non-thermal plasma on particle size distribution and composition of diesel engine particles, *Plasma Sci. Technol.*, Vol. 19 (11), pp. 115503, 2017.
- [19] Gao J., Ma C., Xing S., and Sun L., Oxidation behaviours of particulate matter emitted by a diesel engine equipped with a NTP device, *Appl. Therm. Eng.*, Vol. 119 (5), pp. 593–602, 2017.
- [20] Yao S., Shen X., Zhang X., Han J., Wu Z., Tang X., Lu H., and Jiang B., Sustainable removal of particulate matter from diesel engine exhaust at low temperature using a plasma-catalytic method, *Chem. Eng. J.*, Vol. 327, pp. 343–350, 2017.
- [21] Shi Y., Cai Y., Li X., Ji L., Chen Yi., and Wang W., Evolution of diesel particulate physicochemical properties using nonthermal plasma, *Fuel*, Vol. 253, pp. 1292–1299, 2019.
- [22] Yoshida K., Aftreatment of carbon particles emitted by diesel engine using a combination of corona and dielectric barrier discharge, *IEEE Trans. Ind. Applicat.*, Vol. 55 (5), pp. 5261–5268, 2019.
- [23] Okubo M., Kuroki T., Yoshida K., and Yamamoto T., Single-stage simultaneous reduction of diesel particulate and using oxygen-lean nonthermal plasma application, *IEEE Trans. Ind. Applicat.*, Vol. 46 (6), pp. 2143–2150, 2010.
- [24] Okubo M., Yamada H., Yoshida K., and Kuroki T., Simultaneous reduction of diesel particulate and NO_x using a catalysis-combined nonthermal plasma reactor, *IEEE Trans. Ind. Applicat.*, Vol. 53 (6), 5875–5882, 2017.
- [25] Takehana K., Kuroki T., and Okubo M., Evaluation on nitrogen oxides and nanoparticle removal and nitrogen monoxide generation using a wet-type nonthermal plasma reactor, *J. Phys. D: Appl. Phys.*, Vol. 51 (20), 204002, 2018.